Enhancement of seismic data quality and interpretation for mapping base Zubair sands of Southeast Kuwait

Rajive Kumar[†], Karam, M. Hafez[†], Anandan Mudavakkat[†], Aisha Y. Al-Ghareeb[†], Thekriat Hussain[†], Ritesh K. Sharma[+], and Satinder Chopra[+]*

[†]Kuwait Oil Company, Kuwait; [+]Arcis Seismic Solutions, TGS, Calgary, Canada

Summary

The Lower Zubair sand reservoirs have produced or shown oil in several but not all of the wells drilled in western and southeastern Kuwait. Evidence from the available core and log data analysis suggests that the Lower Zubair sand distribution consists of NE-SW trending estuarine channel fill. Thin due to their strati-structural nature, these Zubair sands are present at some places and absent at others. The tectonic activity in the area has resulted in faults and fractures in the interval comprising not only the Lower Zubair sands but the Middle and Upper Zubair sands as well. In general, the impedance contrast between these thin Zubair sands and the underlying Ratawi shale is poor. Therefore, the challenge is to identify not only the spatial variability of these Lower Zubair sands but also crosscutting faults and fractures. We address these challenges by first enhancing the bandwidth of the available seismic data using spectral inversion to estimate thin bed reflectivity, followed by relative acoustic impedance to map the reservoir heterogeneity, and that in turn followed by coherence and curvature attributes to detect minor faults and fractures.

Introduction

Well W1 which was drilled in 1983 in the Burgan field located in south east Kuwait, led to a chance discovery of hydrocarbon sand at the base of the Zubair Formation. Shortly thereafter, well W2 was drilled targeting the Zubair sand and encountered 18 m of sand completely filled with oil. This success increased the exploration interest in the area and more wells were subsequently drilled. However, well W3 which was drilled just 1.4 km southeast of well W1 encountered thin Zubair sand devoid of hydrocarbons. This was followed with well W4, drilled about 4 km east of well W2, which again came up dry. Well W5 was drilled later and again came up dry. Well W6 is located 1 km west of well W2 and was drilled deeper during 2012. The logging results indicated the basal Zubair sands were wet with just 1 m of oil and some changes in the sand quality as well.

The Zubair Sand Formation is an average of about 460 m thick, and runs through Kuwait. The middle and lower Zubair sand reservoirs have produced hydrocarbons in northern Kuwait. Towards the western and southeastern parts of Kuwait, some wells have produced or shown oil from the lower Zubair sands. Also, in these areas the sand ratio is seen to have increased as compared with the northern part, so that the lesser mudstone content in the Zubair potentially results in discontinuous top seal facies within it from a structural standpoint. Besides this, the core data and log analysis in the southeastern part of Kuwait indicate that the sand distribution is mainly estuarine channel fill in a stratigraphic framework extending in a NE-SW direction. Given this model, it is envisaged that strati-structural traps, ably supported by an effective top seal mechanism, would be suitable for hosting hydrocarbon in lower basal Zubair sands. Such hydrocarbon bearing sands may also be bounded laterally by faults or structural closure elements as has been noticed in the region of interest.

Due to their strati-structural nature, the prospective thin basal Zubair sands show up at some places while at other locations they are absent. Complicating the situation is the fact that the discrimination between those sands and underlying Ratawi shale is poor. So, the challenge in this area is to understand fully the nature of deposition of these basal Zubair sands, their entrapment and the overall play, and be able to identify their spatial variability.

The present study was taken up to address the above objectives. The available seismic data over the area was shot for a shallow objective and its bandwidth was not suitable for detecting the thin sands of interest here. The workflow planned was to first enhance the frequency content of the seismic data by means of spectral inversion as well as use some of the available seismic attributes. Coherence and curvature attributes were used for determining the discontinuities in the data at the target level. Relative acoustic impedance derived from reflectivity was used to characterize the basal Zubair sands. The study has shown the feasibility of such a characterization by following the workflow suggested above.

Geologic setting of the study area

The Great Burgan field in Kuwait is located on the north-south trending Kuwait Arch, believed to be a basement horst reactivated during the Late Jurassic (Carman, 1996) (Figure 1). Three structural culminations give rise to three giant fields, namely Burgan, Magwa and Ahmadi. While the Burgan ovate domal structure lies to the south, the Magwa and Ahmadi are up to the north. Oil has been produced from different formations in these

DOI http://dx.doi.org/10.1190/segam2013-0289.1

structures such as Wara, Mauddud, Burgan and Minagish as indicated in the Lower Cretaceous stratigraphic column shown in Figure 2. Lying above the basal Lower Cretaceous Makhul Formation is the Minagish Formation consisting of argillaceous and oolitic carbonates. It represents good reservoir facies in some areas and is productive in Burgan dome and West Kuwait oil fields. Overlying the Minagish is the Ratawi Formation of Valanginian age. Its lower section is the Ratawi Limestone Member deposited in a shallow gentle ramp setting, while the overlying Ratawi Shale Member deposited in a transgressive episode consists essentially of mainly marine shale/claystone that is interbedded with siltstone and fine-grained sandstone. Above the Ratawi shale lies the regressive clastic dominated Zubair Formation of Berremian age.

Available seismic data

The Burgan field is covered by 3D seismic data of 1997 vintage, but was reprocessed recently. The reprocessing included coherent noise attenuation, surface consistent amplitude compensation and deconvolution, model-based wavelet processing for zero phasing, offset regularization and interpolation, high-resolution Radon multiple attenuation, Kirchhoff time migration and stacking amongst other steps. The data have a bin size of 25m x 25m, a sample interval of 4 ms and a record length of 3s. The quality of the data was reasonable with a bandwidth of 10-60 Hz with a dominant frequency of 30 Hz in the zone of interest, i.e. the Lower Cretaceous succession. If the velocity of the Lower Zubair sands is 3500 m/s, a dominant frequency of 51.5 Hz is required to resolve 17m thick sand. Sand units thinner than this would require higher dominant frequencies for their resolution. Since the data in hand do not have the necessary bandwidth to resolve the Lower Zubair sands, about 400 km^2 of the larger 3D seismic volume was selected for frequency enhancement and other attribute generation.

As stated before, spectral inversion (Chopra et al, 2006) was used to extract thin-bed reflectivity. In addition to extending resolution to ideally resolve the top and bottom of the sand, the thin bed reflectivity was used to generate relative acoustic impedance amplitude (Chopra et al., 2009) that better delineates lateral changes in sand thickness.

The other main objective of this study is to detect minor faults/fractures, which was done by using coherence and curvature attributes. Together, all these attributes were utilized to define the sandstone geometry and distribution of the Lower Zubair incised valleys.

Volumetric estimates of coherence and curvature

As the first step, structure-oriented filtering was run on the input data volume so as to reduce the background noise and so the low coherence or curvature noise on attribute displays (Hoecker and Fehmer, 2001; Chopra and Marfurt, 2007). The parameterization used for these attributes is five samples in the inline, crossline and time directions for computing coherence and three adjacent samples for curvature computation. Time slice displays from the coherence and most-positive and most-negative curvature attributes at the Ratawi level are shown in Figure 3. Fault and fracture lineaments are seen at this level, and looking at the vertical sections, it appears that these discontinuities have an imprint at the Shuaiba level as well.

Thin-bed reflectivity inversion

Thin-bed spectral inversion is a novel way of removing the wavelet from seismic data and extracting reflectivity (Portniaguine and Castagna, 2005; Chopra et al., 2006; Chopra et al., 2008). As described by Puryear and Castagna (2008), the inversion utilizes spectral decomposition to unravel the complex interference patterns created by thin-bed reflectivity. It is based on the premise that the spacing between spectral peaks and notches for a windowed portion of a seismic trace is a function of layer thickness in the time domain (Partyka et al., 1999). In the special case of a seismic reflection response produced by a single layer and, in the absence of noise, it is possible to determine layer thickness uniquely with no resolution limit by inverting a relatively narrow band of frequencies (where the top and base reflection coefficients have unknown polarities and magnitudes) provided that the wavelet spectrum is known and there is an even component to the reflection response (Chopra et al., 2006). Under such circumstances, once layer thickness is found, both top and base reflection coefficients can also be determined. In practice, thickness and reflection coefficients can be inverted for as far below the tuning thickness as noise will allow.

Before running the thin-bed reflectivity inversion on the data, well log correlation with input seismic data was carried out for the different wells. The synthetic seismograms showed a reasonable matching with the seismic data at the main markers, and somewhat weaker matching at the intermediate levels. Thin-bed reflectivity was run on data which had been passed through structure-oriented filtering. A segment of the input seismic data is shown in Figure 4a, and the derived thin-bed reflectivity provides considerable detail as shown in Figure 4b.

Horizons picked on coherent reflectors on the input seismic data, seemed to match the reflectivity well, but horizons picked on not-so-coherent reflectors in the input seismic data appeared as irregular and erroneous on the reflectivity. We therefore autopicked the horizons on the smoothed reflectivity to get them tracked with accuracy. Horizon slices generated from the coherence and curvature attribute volumes using reflectivity tracked horizons depicted the different features seen on these displays clearer than before. Apart from this advantage, one significant benefit of deriving the high-resolution reflectivity from seismic data is that it is now possible to filter it back to a

DOI http://dx.doi.org/10.1190/segam2013-0289.1

bandwidth that is higher than the input data. With this in mind the derived reflectivity was filtered to a bandwidth of 10-120 Hz (found suitable as per the quality of the data), and then correlated with the available log control. The filtered thin-bed reflectivity and its correlation with impedance log curves is showsn in Figure 5. While the correlation is good, it was found that this bandwidth was not enough to resolve the sand thickness. With this discouraging observation, we went on to invoke our alternative approach – that of interpreting sands via their associated amplitudes and as isochron units.

Relative acoustic impedance from thin-bed reflectivity

Interpretation of seismic data is usually carried out on vertical profiles (inlines and crosslines) in preference to time or horizon slices. Correlation of top and base of thin layers with their respective changes on log curves could be time consuming and laborious, especially if there is an abundance of thin layers to be correlated. A way out of this problem is to integrate the thin-bed reflectivity to produce a band-limited impedance estimate that is unbiased by existing well information. Such displays are useful for correlating the different horizon intervals corresponding to subsurface rock intervals with the individual litho-units interpreted on log curves. Time or horizon slices from impedance volumes serve as useful displays for stratigraphic differentiation of different strata. The thin-bed impedance showed the features much better in their definition, clarity and resolution. A horizon slice from the relative acoustic impedance derived from the thin-bed reflectivity, in an 8 ms interval above the Ratawi horizon is shown in Figure 6. Notice the signature of the Zubair sands seen in brown, not as a single body, but as a scattered distribution of high impedance patterns which appear meaningful. These patterns could be interpreted as the presence of the Zubair sand in a background of shale.

Seismic facies by impedance waveform classification

The shape and character of the seismic waveform is often used to characterize reservoir quality. This is because the waveform carries information about the phase, frequency and amplitude – and any variation in these parameters is considered reflective of the lateral variations in lithology, porosity and fluid content. So, if the shape and character of seismic waveforms in a given target zone are studied using some pattern recognition type of a process, and then displayed in a map view, the display would indicate seismic facies variation at the target level. One approach to pattern recognition is with the use of neural networks to compare seismic waveforms and group them into different classes. Usually, without any external input, such an approach is referred to as unsupervised waveform classification.

In the case at hand, we performed unsupervised waveform classification on relative acoustic impedance data in the thin zone enclosing the Zubair sands. The waveform classification result is shown in Figure 7, and the patterns match very closely the sand distribution map generated from relative acoustic impedance shown in Figure 6.

Conclusions

The present study helped in achieving the goals set for the exercise and the following main conclusions could be drawn.

1. The application of coherence and curvature attributes on the input seismic data indicates fault lineaments as well as fracture lineament trends clearly at the Ratawi level and other levels of interest. Such attributes displayed alone as well as in combination yield meaningful information.

2. Due to the poor resolution of the input data, thin-bed reflectivity run on the input data furnished more reflectivity detail. This was also supplemented with a higher resolution filtered reflectivity volume and the relative acoustic impedance. It was found that the Zubair sands show only localized signatures above the Ratawi marker and they were not amenable to picking.

3. Relative acoustic impedance exhibited sand signatures just above the Ratawi horizon and so horizon map was prepared by averaging the relative acoustic impedance in a 8ms window above the horizon. This map indicates the distribution of the Zubair sands, and matches a similar map prepared by using seismic waveform classification.

On the whole, the application of coherence/curvature attributes as well as thin-bed reflectivity inversion on the input seismic data, enabled getting a detailed understanding of the discontinuities and enhancing the resolution of the data which was the main objective of the exercise.

Acknowledgements

The authors extend sincere thanks to the Ministry of Oil, State of Kuwait and the Kuwait Oil Company for granting permission to publish this work. Suggestions from colleagues for improvement of quality of this paper are also greatly appreciated. The thin-bed reflectivity discussed in this paper is commercially referred to as ThinMAN™.

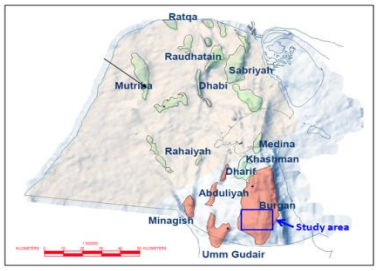

Figure 1: Index map showing the major Cretaceous oils fields of Kuwait. The blue rectangle shows the area over which the study was carried out.

DOI http://dx.doi.org/10.1190/segam2013-0289.1

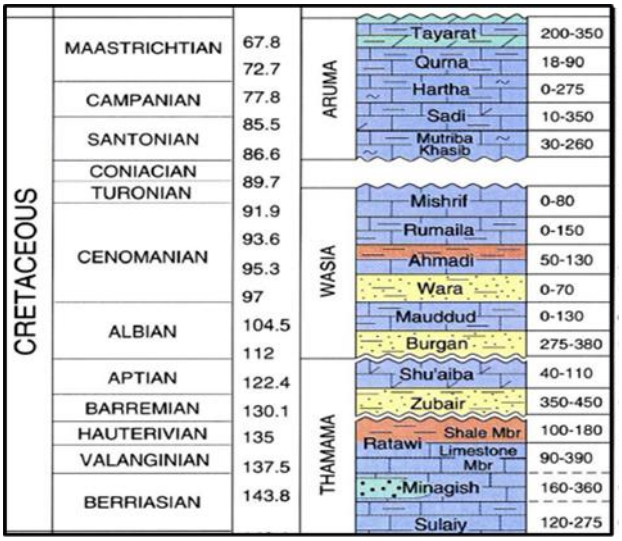

Figure 2: Stratigraphic column for the area under study.

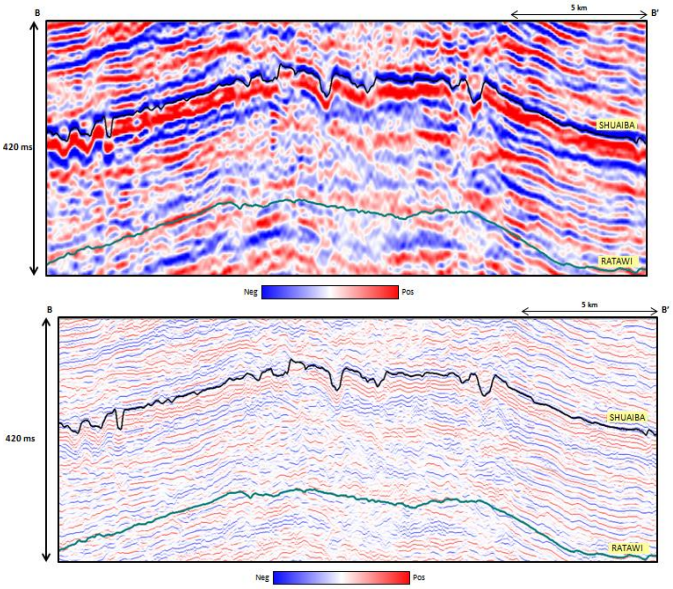

Figure 4: A segment of a seismic section from an inline from (above) input data, and (b) the filtered thin-bed reflectivity volume with a bandpass higher than the input data bandwidth (10-120 Hz). The Shuaiba (upper) and the Ratawi (lower) markers are shown overlaid on it.

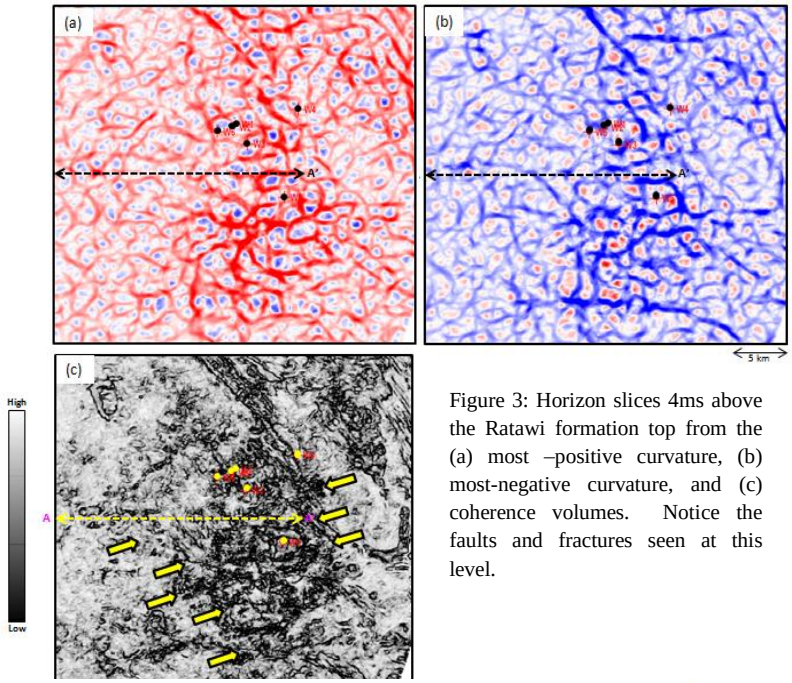

Figure 3: Horizon slices 4ms above the Ratawi formation top from the (a) most –positive curvature, (b) most-negative curvature, and (c) coherence volumes. Notice the faults and fractures seen at this level.

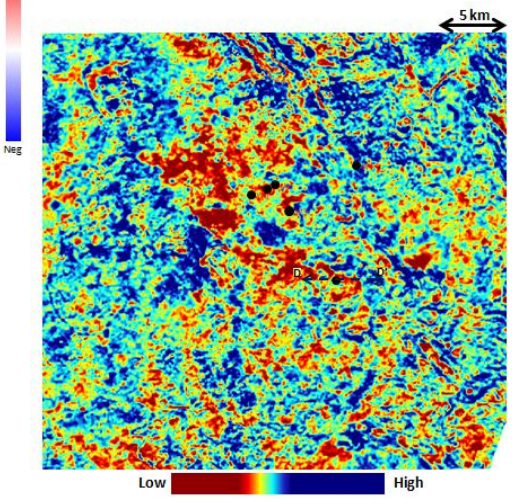

Figure 6: Thin-bed relative acoustic impedance strat-slice 8 ms above the Ratawi horizon showing the signature of the Zubair sands in brown.

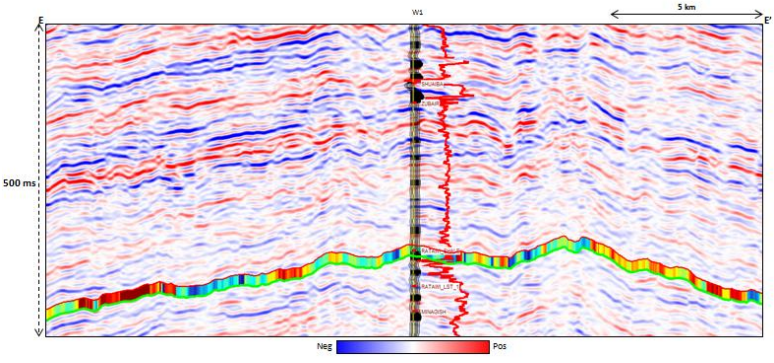

Figure 5: Correlation of log curve from W1 with filtered thin-bed reflectivity and an overlay of strata grid from thin-bed relative acoustic impedance. Notice the lateral variation of the impedance within the thin zone that encompasses the Zubair sands.

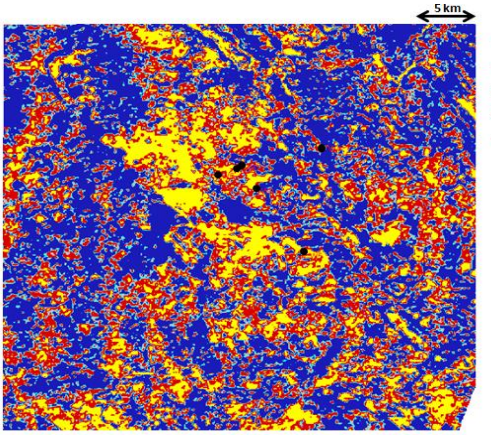

Figure 7: Unconstrained facies classification derived from thin-bed relative acoustic impedance which uses neural networks.

DOI http://dx.doi.org/10.1190/segam2013-0289.1

http://dx.doi.org/10.1190/segam2013-0289.1

EDITED REFERENCES

Note: This reference list is a copy-edited version of the reference list submitted by the author. Reference lists for the 2013 SEG Technical Program Expanded Abstracts have been copy edited so that references provided with the online metadata for each paper will achieve a high degree of linking to cited sources that appear on the Web.

REFERENCES

Al-Dossary, S., and K. J. Marfurt, 2006, Multispectral estimates of reflector curvature and rotation: Geophysics, **71**, no. 5, P41–P51, http://dx.doi.org/10.1190/1.2242449.

Carman, G. J., 1996, Structural elements of onshore Kuwait: GeoArabia, **1**, no. 2, 239–266.

Chopra, S., J. P. Castagna, and O. Portniaguine, 2006, Seismic resolution and thin-bed reflectivity inversion: CSEG Recorder, **31**, no. 1, 19–25.

Chopra, S., J. P. Castagna, and Y. Xu, 2008, When thin is in, enhancement helps: AAPG Explorer, http://www.aapg.org/explorer/geophysical_corner/2008/05gpc.cfm.

Chopra, S., J. P. Castagna, and Y. Xu, 2009, Thin is in: Here's a helpful attribute: AAPG Explorer, http://www.aapg.org/explorer/2009/07jul/gpc0709.cfm.

Chopra, S., and K. J. Marfurt, 2007, 3D seismic attributes for prospect generation and reservoir characterization: SEG.

Hoecker, C., and G. Fehmers, 2002, Fast structural interpretation with structure-oriented filtering: The Leading Edge, **21**, 238–243, http://dx.doi.org/10.1190/1.1463775.

Partyka, G. A., J. Gridley, and J. Lopez, 1999, Interpretational applications of spectral decomposition in reservoir characterization: The Leading Edge, **18**, 353–360, http://dx.doi.org/10.1190/1.1438295.

Portniaguine, O., and J. P. Castagna, 2005, Spectral inversion: Lessons from modeling and Boonesville case study: 75th Annual International Meeting, SEG, Expanded Abstracts, 1638–1641.

Puryear, C. I., and J. P. Castagna, 2008, Layer-thickness determination and stratigraphic interpretation using spectral inversion: Theory and application: Geophysics, **73**, no. 2, R37–R48, http://dx.doi.org/10.1190/1.2838274.